Short communication

Structural and electrochemical properties of nanocomposites formed by V_2O_5 and poly(3-alkylpyrroles)

Fritz Huguenin[a], Emerson M. Girotto[b], Giacomo Ruggeri[c], Roberto M. Torresi[d,*]

[a]*Instituto de Química de São Carlos, Universidade de São Paulo, CP 780, 13560-970 São Carlos, SP, Brazil*
[b]*Departamento de Química, Universidade Estadual de Maringá, Av. Colombo 5790, 87020-900 Maringá, PR, Brazil*
[c]*Dipartimento di Chimica e Chimica Industriale, Università di Pisa, via Risorgimento 35, I-56126 Pisa, Italy*
[d]*Instituto de Química, Universidade de São Paulo, CP 26077, 05513-970 São Paulo, SP, Brazil*

Abstract

Synthesis and characterisation of new nanocomposites of poly(3-decylpyrrole) (P3DP) and poly(hexadecylpyrrole) (P3HDP) with V_2O_5 are described. These nanocomposites were characterised using X-ray diffraction (XRD), electrochemical quartz crystal microbalance, electroacoustic impedance (EAI) and cyclic voltammetry. The results were compared with an other nanocomposite, polypyrrole (Ppy)/V_2O_5, aiming to verify the influence of the side chains of P3DP and P3HDP on the electrochemical behaviour of V_2O_5. These hybrid materials have different structures that modify the electrochemical properties. The side chains of P3DP and P3HDP contributed to greater electrochemical stability than that of Ppy into the V_2O_5 matrix. This results in a higher specific capacity for the P3DP/V_2O_5 and P3HDP/V_2O_5 nanocomposites (115 and 106 Ah kg^{-1}, respectively) than that of Ppy/V_2O_5 (50 Ah kg^{-1}) after 50 electrochemical cycles.
© 2002 Published by Elsevier Science B.V.

Keywords: Vanadium pentoxide; Polypyrrole; Polypyrrole derivatives; Nanocomposites

1. Introduction

In the last year, several groups have reported important results on nanoscience and nanotechnology. The design of nanoscale objects can optimise several properties, in optics, electronics, catalysis, biotechnology, etc. [1]. In addition, the design of nanohybrid architectures have been explored as cathode materials for Li-ion batteries. Hybrid materials formed by an intimate contact at molecular level between electronic conducting polymers (ECP) and vanadium pentoxide (V_2O_5) [2–17] are excellent candidates for this category of cathodes. Specifically, the nanocomposite formed by polypyrrole (Ppy) and V_2O_5 has shown a higher specific capacity and energy density than that of the xerogel film [5,7,8]. However, the present work shows that the Ppy/V_2O_5 nanocomposite shows an important electrochemical instability when cycled several times, making its practical use unsatisfactory. One approach to addressing this issue is to intercalate polypyrrole derivatives into the oxide, as poly(3-alkylpyrrole) [18,19], since they offer the possibility of

alleviating structural changes during the redox process due to their side chain length.

In this work, the structural, mechanical and electrochemical properties of the Ppy/V_2O_5 nanocomposite and novel nanocomposites with V_2O_5, poly(3-decylpyrrole) (P3DP)/V_2O_5 and poly(hexadecylpyrrole) (P3HDP)/V_2O_5 were examined. These properties were investigated using X-ray diffraction (XRD), electroacoustic impedance (EAI), electrochemical quartz crystal microbalance (EQCM) and cyclic voltammetry.

2. Experimental

The nanocomposites of Ppy/V_2O_5, P3DP/V_2O_5 and P3HDP/V_2O_5 were produced by addition of 1.42×10^{-4} mol of pyrrole (Aldrich, previously distilled), 3DP and 3HDP (monomers prepared according to [20,21]) to 120 ml of water. Soon after, 8.5×10^{-4} mol of vanadyl tris(isopropoxide), $VC_9H_{21}O_4$ (Gelest), was added to this solution giving a green transparent liquid. The volume was then reduced by heating under vacuum in the temperature range of 55–70 °C using a rotary evaporator during a period of ca. 2 h. This procedure results in the reduction of a fraction of

* Corresponding author. Tel.: +55-11-3091-2165;
fax: +55-11-3815-5579.
E-mail address: rtorresi@iq.usp.br (R.M. Torresi).

the vanadium(V) species to vanadium(IV) with a consequent oxidative polymerisation of the monomers. To prepare thin films, the resulting solution was dropped onto appropriate substrates and then evaporated by heating at 100 °C for 2 h.

X-ray diffraction measurements were run in a Carl Zeiss URD-6 diffractometer using monochromatic Cu Kα radiation. The samples were thin, cast films of the nanocomposite on ITO substrates. For electrochemical experiments, the counter electrode was platinum and the reference was Ag | AgNO$_3$ saturated. The substrates of the working electrodes were 6 MHz AT-cut quartz crystals coated with gold by thermal vacuum deposition, followed by electrodeposition of Pt from a solution of H$_2$PtCl$_6$. The piezoelectrically and electrochemically active area was 0.31 cm^2 with an integral sensitivity constant, K, of 6.45×10^7 cm^2 s^{-1} g^{-1} (experimentally determined for the electrodes used in this work [22]). The resonance frequency shift was measured with a HP-5370B Universal Timer/Counter. Electrochemical measurements were carried out using a FAC 2001 potentiostat/galvanostat. Changes in the resonance frequency of the EQCM crystal were transformed into mass changes by using the Sauerbrey equation [23]. Electroacoustic impedance measurements were made with a HP-4192A Frequency Impedance Meter.

3. Results and discussion

Fig. 1 shows the X-ray diffraction data for [Ppy]$_{0.3}$V$_2$O$_5$, [P3DP]$_{0.3}$V$_2$O$_5$ and [P3HDP]$_{0.3}$V$_2$O$_5$. The curve for [Ppy]$_{0.3}$V$_2$O$_5$ clearly shows some (0 0 1) peaks, typical of turbostratic stacking of the dimeric V$_2$O$_5$ slabs. The 2θ value of the (0 0 1) plane corresponds to an interplanar spacing of 1.38 nm, consistent with previous reports on Ppy/V$_2$O$_5$ hybrid materials [5]. This spacing suggests that at least some of the Ppy fraction intercalates into turbostratic stacking of V$_2$O$_5$, indicating an intimate contact between the electronic conducting polymer and the host matrix in this material, called a nanocomposite. Curiously, with a peak associated to the (0 0 2) plane, which is not observed for V$_2$O$_5$ xerogel [13] was found. The discussion of the structure of V$_2$O$_5$ is reported elsewhere [24,25], and the absence of this peak suggests that this material is formed by the stacking of V$_2$O$_5$ bilayers [24,26]. Thus, XRD data show that the presence of Ppy modifies the structure of the inorganic matrix, which must be formed by the stacking of monolayers. The weakness and width of the (0 0 1) signals for [Ppy]$_{0.3}$V$_2$O$_5$ suggests a poorly organised structure compared with V$_2$O$_5$ [13]. This is ascribed to a decrease in the length of the oxide chains provided by the presence of Ppy during the condensation process [7]. The curves for [P3DP]$_{0.3}$V$_2$O$_5$ and [P3HDP]$_{0.3}$V$_2$O$_5$ also show an interplanar spacing of 1.38 nm, consistent with the intercalation of P3DP and P3HDP between the lamellae of V$_2$O$_5$. However, the alkyl chains linked to the pyrrole ring do not contribute to the increase of the interlayer space. This fact
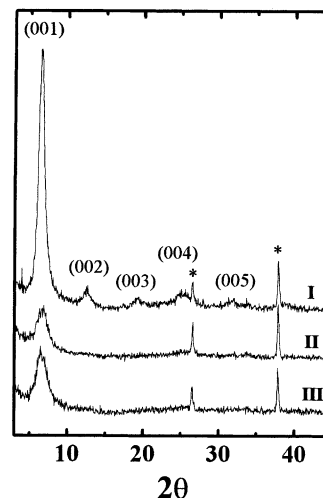

Fig. 1. X-ray diffraction patterns of [Ppy]$_{0.3}$V$_2$O$_5$ (I), [P3DP]$_{0.3}$V$_2$O$_5$ (II) and [P3HDP]$_{0.3}$V$_2$O$_5$ (III). The signal ($*$) is associated to peaks of the substrate. The crystallographic planes corresponding to the characteristic peaks are also shown.

suggests that the plane of the pyrrole rings is parallel to the (0 0 1) planes. Moreover, it is observed an increase in amorphicity compared to the [Ppy]$_{0.3}$V$_2$O$_5$. This increase in the structural disorder can be assigned to the alkyl chains, which provides a considerably decreasing length of the oxide chains.

In order to investigate the influence of these distinct polymers on the viscoelastic properties of the nanocomposites and to validate Sauerbrey's equation, electroacoustic impedance experiments were examined. Firstly, 0.4 V (oxidised state) was applied for a half-hour, allowing the system to reach electrochemical equilibrium. After-wards, this procedure was repeated at −1.2 V (reduced state). The EAI data were obtained between 5.895 and 5.905 MHz. Small changes in the conductance and half-band width values were observed from the oxidised state to the reduced state for all studied nanocomposites. Specifically, there was a decrease in the conductance values of 2.7% (from 1.346 to 1.310 ms), 0.5% (from 0.796 to 0.792 ms) and 1.9% (from 0.855 to 0.839 ms) for [Ppy]$_{0.3}$V$_2$O$_5$, [P3DP]$_{0.3}$V$_2$O$_5$ and [P3HDP]$_{0.3}$V$_2$O$_5$, respectively. In addition, there was an increase in half-band width values of 3.5% (from 2261 to 2340 Hz), 2.3% (from 4047 to 4142 Hz) and 1.1% (from 4090 to 4135 Hz) for [Ppy]$_{0.3}$V$_2$O$_5$, [P3DP]$_{0.3}$V$_2$O$_5$ and [P3HDP]$_{0.3}$V$_2$O$_5$, respectively. Although these experiments cannot distinguish the mechanical properties among the studied nanocomposites, they can be used to assign a better mechanic stability in comparison with V$_2$O$_5$ xerogel. In fact, the EAI data of V$_2$O$_5$ xerogel show significant changes from oxidised to reduced states [17]. These results confirm the validity of Sauerbrey's equation. So, frequency change can be transformed in mass changes for these hybrid nanocomposites.

Fig. 2 shows $\Delta m/E$ and $\Delta m_c/E$, where Δm_c was determined by considering only the intercalation/deintercalation
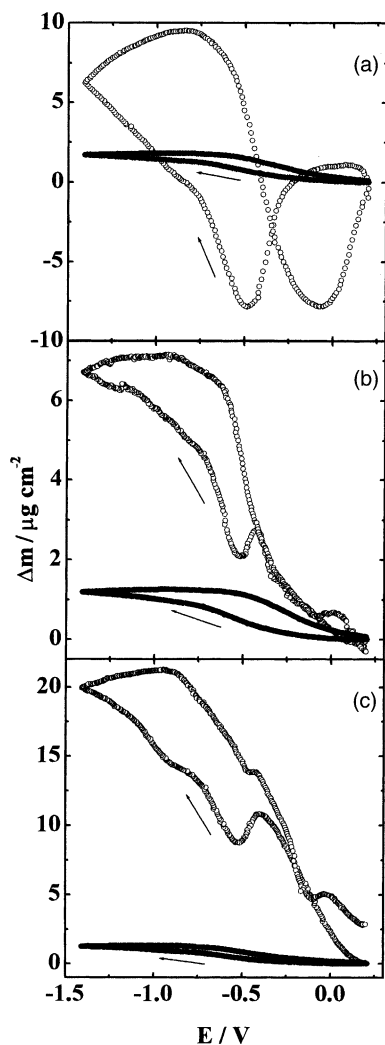
Fig. 2. The (●) calculated and (○) experimental $\Delta m/E$ potentiodynamic profiles of (a) $[Ppy]_{0.3}V_2O_5$; (b) $[P3DP]_{0.3}V_2O_5$ and (c) $[P3HDP]_{0.3}V_2O_5$ in $LiClO_4$ 0.5 mol l^{-1}/PC electrolytic solution. Scan rate = 0.005 V s^{-1}.

Fig. 3. The (●) 3rd and (○) 50th voltammetric cycle of (a) $[Ppy]_{0.3}V_2O_5$, (b) $[P3DP]_{0.3}V_2O_5$ and (c) $[P3HDP]_{0.3}V_2O_5$ in $LiClO_4$ 0.5 mol l^{-1}/PC electrolytic solution. Scan rate = 0.005 V s^{-1}. Film mass = 16 μg.

of Li$^+$ ions, transforming charge in mass. The experimental results were recorded when the mass shift was invariant with time. Experimental mass change is in all cases larger than the calculated one suggesting that a significant amount of solvent molecules intercalates/deintercalates into the host matrixes. Moreover, a different profile for $[Ppy]_{0.3}V_2O_5$ (Fig. 2a) in comparison to $[P3DP]_{0.3}V_2O_5$ (Fig. 2b) and $[P3HDP]_{0.3}V_2O_5$ (Fig. 2c) was observed. For $E > -0.5$ V, a significant mass decrease during negative potential scan is attributed to deintercalation of solvent molecules, similar to EQCM data for V_2O_5 [27]. The opposite process was observed during positive potential scan. For all the nanocomposites, the mass increase (decrease) during the negative (positive) potential scan is associated with intercalation (deintercalation) of Li$^+$ and solvent molecules. The participation of ClO_4^- in the charge compensation mechanism should give a mass shift profile opposite to that observed [28]. This fact indicates that oxide chains act as counter-anions
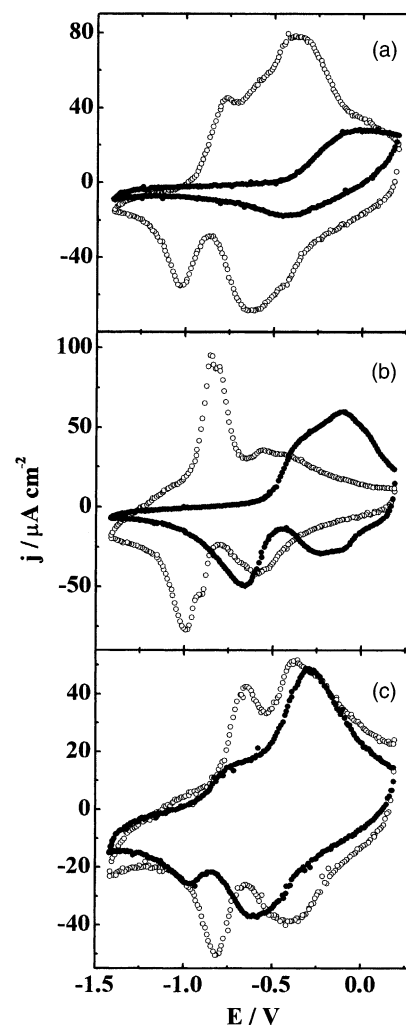
for the electronically conducting polymers, suggesting an intimate contact between organic and inorganic materials in the ordered and amorphous parts of the films. The difference in the intercalation process of solvent molecules can be associated the morphology of these materials. For composites formed by V_2O_5 with low ordered lamellae, as PANI/V_2O_5 [17] and PSPAN/V_2O_5 [29], a significant expulsion (incorporation) of solvent (in this case propylene carbonate) during the intercalation (deintercalation) of Li$^+$ was not seen.

An essential characteristic of these types of materials is electrochemical stability, because these materials are subjected to multiple charge/discharge cycles. Fig. 3 shows the 3rd and 50th voltammetric cycles for $[Ppy]_{0.3}V_2O_5$, $[P3DP]_{0.3}V_2O_5$ and $[P3HDP]_{0.3}V_2O_5$. For the third cycle, it was found a greater specific capacity for $[Ppy]_{0.3}V_2O_5$ (198 Ah kg^{-1}) compared to $[P3DP]_{0.3}V_2O_5$ (150 Ah kg^{-1}) and $[P3HDP]_{0.3}V_2O_5$ (148 Ah kg^{-1}). However, the specific

capacity of $[Ppy]_{0.3}V_2O_5$ decreased to 50 Ah kg^{-1} (25% of charge injected in third cycle) after 50 cycles. This is in contrast to the other nanocomposites, i.e. the $[P3DP]_{0.3}V_2O_5$ and $[P3HDP]_{0.3}V_2O_5$ which retain specific capacity, 115 and 106 Ah kg^{-1} (76 and 72%, respectively of charge injected in the third cycle) after 50 cycles. Another important observation is the change observed in the current–potential profile. The third potentiodynamic cycle for $[Ppy]_{0.3}V_2O_5$ is markedly changed after 50 cycles, showing a significant potential peak shift to more positive values. Otherwise, the $[P3HDP]_{0.3}V_2O_5$ nanocomposite shows a better electrochemical stability. For some insertion electrodes, the stability depends on structural changes during the redox process. It is known that the electrochemical profile of V_2O_5 xerogel changes during the intercalation/deintercalation of Li$^+$ due to structural changes [30]. Thus, the voltammograms shown in Fig. 3 indicate that the alkyl chains (mainly from the P3HDP polymer) avoid significant structural modifications, contributing to a greater electrochemical stability of $[P3DP]_{0.3}V_2O_5$ and $[P3HDP]_{0.3}$-V_2O_5 than that of $[Ppy]_{0.3}V_2O_5$.

4. Conclusions

The synthesis method employed in this work, allowed the formation of thin homogeneous films. The XRD and EQCM data have shown that the inorganic and organic components are intimately mixed in the crystalline and amorphous regions. The participation of anions for charge compensation mechanism in these materials, was not observed, suggesting that the V_2O_5 matrix acts as a "counter-anion" for the organic polymers This is very important because it minimises the amount of electrolyte required in Li-ion batteries, increasing the specific capacity of the device. The presence of ECP avoids significant changes in the viscoelastic properties and modifies the V_2O_5 matrix structure, altering the intercalation mechanism of solvent molecules. In addition, the presence of long alkyl chains linked to pyrrole ring avoids significant dimensional changes of the V_2O_5 matrix, assuring a higher electrochemical stability than that of the $[Ppy]_{0.3}V_2O_5$. However, it is still necessary to better understand these materials, for optimisation of their use in Li-ion batteries.

Acknowledgements

References

[1] E. Bourgeat-Lami, J. Nanosci. Nanotechnol. 2 (2002) 1.
[2] Y.-J. Liu, D.C. DeGroot, J.L. Schindler, C.R. Kannewurf, M.G. Kanatzidis, J. Chem. Soc., Chem. Commun. (1993) 593.
[3] V.D. Pokhodenko, V.G. Koshechko, V. Kiylov, J. Power Sources 45 (1993) 1.
[4] F. Leroux, B.F. Koene, L.F. Nazar, J. Electrochem. Soc. 143 (1996) L181.
[5] F. Leroux, G. Goward, W.P. Power, L.F. Nazar, J. Electrochem. Soc. 144 (1997) 3866.
[6] J. Harreld, H.P. Wong, B.C. Dave, B. Dunn, L.F. Nazar, J. Non-Cryst. Solids 225 (1998) 319.
[7] H.P. Wong, B.C. Dave, F. Leroux, J. Harreld, B. Dunn, L.F. Nazar, J. Mater. Chem. 8 (1998) 1019.
[8] G.R. Goward, F. Leroux, L.F. Nazar, Electrochim. Acta 43 (1998) 1307.
[9] G.J.F. Demets, F.J. Anaissi, H.E. Toma, Electrochim. Acta 46 (2000) 547.
[10] J. Wang, K.E. Gonsalves, J. Comb. Chem. 1 (1999) 216.
[11] M. Lira-Cantú, P. Gómez-Romero, J. Electrochem. Soc. 146 (1999) 2029.
[12] E. Shouji, D.A. Buttry, Langmuir 15 (1999) 669.
[13] F. Huguenin, M.T. do Prado Gambardella, R.M. Torresi, S.I. Córdoba de Torresi, D.A. Buttry, J. Electrochem. Soc. 147 (2000) 2437.
[14] H.P. Oliveira, C.F.O. Graeff, C.A. Brunello, E.M. Guerra, J. Non-Cryst. Solids 273 (2000) 193.
[15] W. Chun-Guey, H. Jiunn-Yih, H. Shui-Sheng, J. Mater. Chem. 11 (2001) 2061.
[16] M. Ferreira, V. Zucolotto, F. Huguenin, R.M. Torresi, O.N. Oliveira Jr., J. Nanosci. Nanotechnol. 2 (2002) 1.
[17] F. Huguenin, R.M. Torresi, D.A. Buttry, J. Electrochem. Soc. 149 (2002) A546.
[18] N. Constantini, R. Cagnolati, L. Nucci, F. Pergola, G. Ruggeri, Synth. Met 92 (1998) 139.
[19] N. Constantini, S. Capaccioli, M. Geppi, G. Ruggeri, Polym. Adv. Technol. 11 (2000) 27.
[20] J. Rühe, T.A. Ezquerra, G. Wegner, Synth. Met. 28 (1989) C177.
[21] G. Ruggeri, E. Spila, G. Puncioni, F. Ciardelli, Macromol. Rapid. Commun. 15 (1994) 537.
[22] C. Gabrielli, M. Keddam, R. Torresi, J. Electrochem. Soc. 138 (1991) 2657.
[23] G. Sauerbrey, Z. Phys. 155 (1959) 206.
[24] T. Yao, Y. Oka, N. Yamamoto, Mater. Res. Bull. 27 (1992) 669.
[25] J. Livage, Coord. Chem. Rev. 190–192 (1999) 391.
[26] F.J. Anaissi, G.J.F. Demets, E.B. Alvarez, M.J. Politi, H.E. Toma, Electrochim. Acta 47 (2001) 441.
[27] F. Huguenin, M.J. Giz, E.A. Ticianelli, R.M. Torresi, J. Power Sources 103 (2001) 113.
[28] K. Naoi, M.M. Lien, W.H. Smyrl, J. Electroanal. Chem. 272 (1989) 273.
[29] F. Huguenin, R.M. Torresi, D.A. Buttry, J.E. Pereira da Silva, S.I. Córdoba de Torresi, Electrochim. Acta 46 (2001) 3555.
[30] J.-P. Pereira-Ramos, N. Baffier, G. Pistoia, in: G. Pistoia (Ed.), Lithium Batteries—New Materials, Developments and Perspectives, Elsevier, Amsterdam, 1994, p. 281.